Chemistry–A European Journal

Research Article
doi.org/10.1002/chem.202401987

Chemistry Europe
European Chemical Societies Publishing

www.chemeurj.org

Mausolates: Large-Cavity Chelates with Potential as Delivery Vehicles in Nuclear Medicine**

Amanda J. Ackroyd,[a] Leah Gajecki,[a] Athan T. Gogoulis,[a] Jack F. Smart,[a] Allen G. Oliver,[b] J. Scott McIndoe,[a] and David J. Berg*[a]

Dedicated to the memory of Professor Richard A. Andersen

A new type of diborate clathrochelate (cage) ligand featuring nine inwardly pointing nitrogen donors that form a large, rigid cavity, termed a mausolate, is presented. The cavity size and high denticity make this an attractive delivery vehicle for large radionuclides in nuclear medicine. Metal mausolate complexes are stable to air and water (neutral pH) and display extremely high thermal stability (>400 °C). Lanthanide uptake by the mausolate ligand occurs rapidly in solution at room temperature and once complexed, the lanthanide ions are not displaced by a 250-fold excess of a competitive lanthanide salt over more than one week.

Targeted radiotherapy is increasingly used in the treatment of cancer and many of the most important radionuclides are those of large metals including the lanthanides and actinides.[1–5] Targeted alpha therapy (TAT) using ^{225}Ac ($t_{1/2}$, 10.0d), ^{227}Th (18.5d) and ^{223}Ra (11.4d) radionuclides are especially interesting because they possess half-lives of sufficient length for monoclonal antibody targeting.[6–9] Despite these advantages, developing new TAT agents based on these metals is limited by the high lability of their complexes with traditional chelating ligands.

We report here a new class of clathrochelate (*i.e.* cage) that offers exceptional promise as a chelator for very large cations due to its large internal cavity, high denticity and rigid framework (Figure 1).[10] The core structure is based on *tris*(pyrazolyl)borate units connected through pyridine linkers to form a cage. Despite the fact that *tris*(pyrazolyl)borates have been one of the most important ligand classes in inorganic chemistry since their synthesis by Trofimenko in the 1960's, no cage ligands based on this structural core are known.[11–17] The diborate cages described here, which we term mausolates (from mausoleum, a large tomb, in an extension to the well-known and smaller sepulchrates and cryptands), are easy to prepare, show exceptional stability to water and are thermally stable to more than 400 °C.

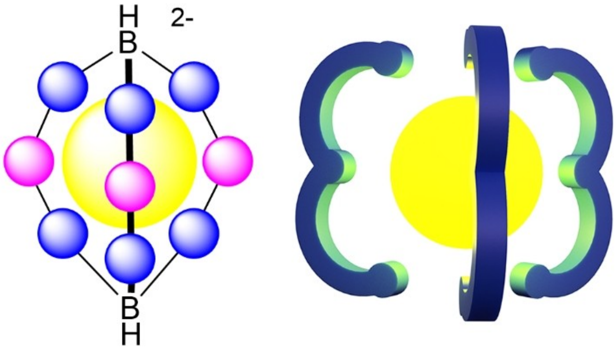

Figure 1. Schematic drawing of the new cage ligand presented here (blue, pyrazolyl-N; pink, pyridine-N; yellow, large encapsulated metal ion).

The synthesis of the *bis*(pyrazolyl)pyridine 'arms' from 2,6-diacetylpyrdine is shown in Scheme 1. The 5′-methylpyrazole derivative **2b** can be made by substituting dimethylacetamide dimethylacetal (DMAc-DMA) for dimethylformamide dimethylacetal (DMF-DMA). Reaction of the arms with KBH_4 in a 3:2 ratio can be carried out in the melt or in solution (diglyme or anisole at 160 °C) to produce the dipotassium salt of the cage (**3a** or **3b**). We have found that a small amount of $Y(OTf)_3$ (*ca.* 2–5 mol%) increases the rate of mausolate formation and provides somewhat higher yield (see *Supporting Information*). Yields as high as 60–70% can be obtained in solution but this method requires the removal of diglyme or anisole at >100 °C under vacuum. The solid state reaction gives more variable yields but 30–50% is typical. Interestingly, the yield is markedly lower if $NaBH_4$ is used and very little product forms with $LiBH_4$, providing some evidence for a potassium ion template effect.

The dipotassium cage complexes **3a** and **3b** are readily soluble in acetone, acetonitrile, THF, methanol and dmso but

---

[a] A. J. Ackroyd, L. Gajecki, A. T. Gogoulis, J. F. Smart, J. S. McIndoe, D. J. Berg
Department of Chemistry, University of Victoria, P.O. Box 1700 Stn CSC, Victoria, BC V8W 2Y2 Canada
E-mail: djberg@uvic.ca

[b] A. G. Oliver
Department of Chemistry and Biochemistry, University of Notre Dame, Notre Dame, IN 46556 USA

[**] From mausoleum: a large tomb; in the spirit of sepulchrates and cryptands.

Supporting information for this article is available on the WWW under https://doi.org/10.1002/chem.202401987

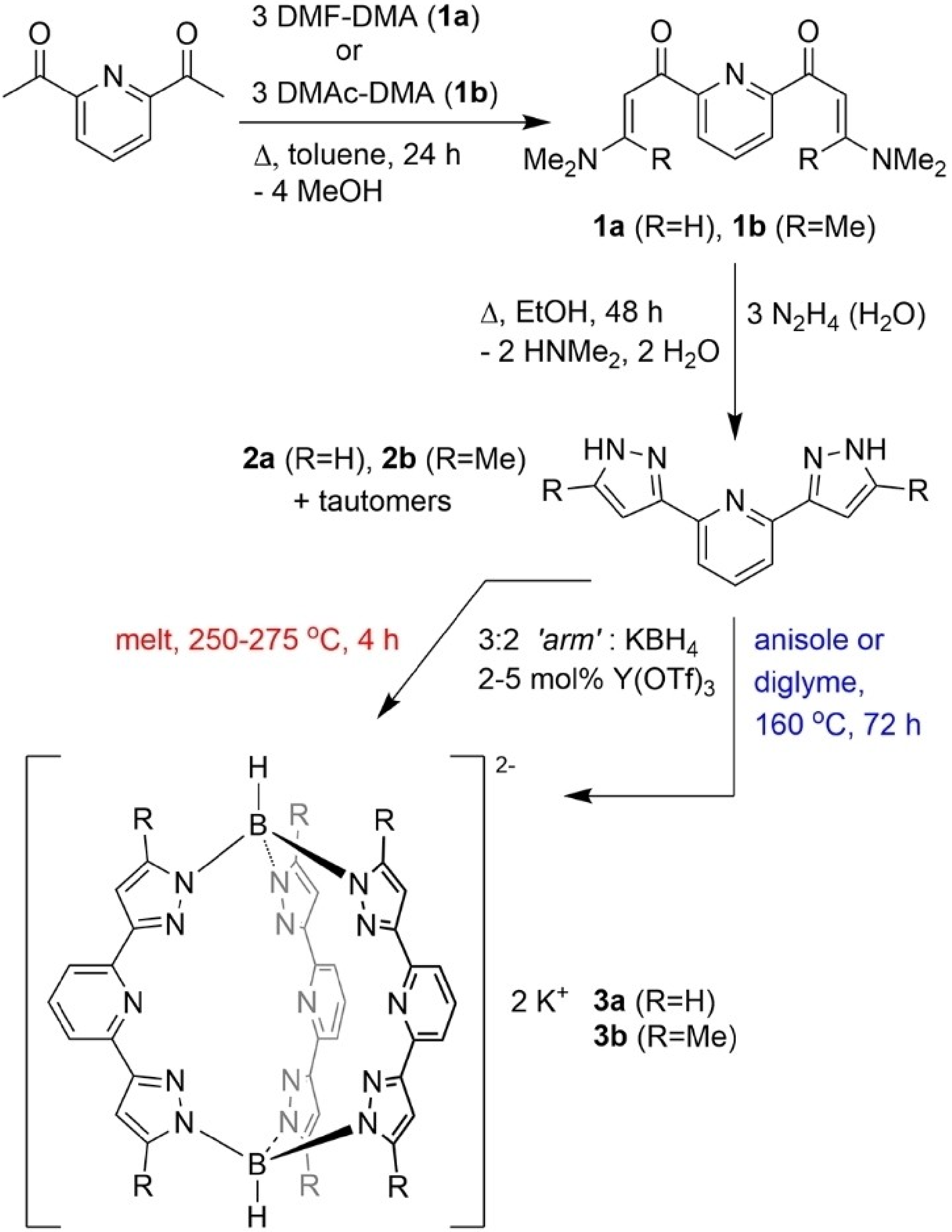

Scheme 1. Synthesis of the dipotassium salts of mausolates **3 a** and **3 b**.

are insoluble in water. The NMR spectra of these complexes are highly symmetrical in acetone-d_6 or dmso-d_6 and, unlike the tautomeric arms **2 a** and **2 b**, display sharp signals for the pyrazolyl protons with the characteristic 2–3 Hz $^3J_{HH}$ pyrazole coupling (for **3 a**). The B*H* resonance near 4.9 ppm is a very broad multiplet in acetone-d_6 in the ^{1}H NMR but sharpens considerably to a broad singlet on ^{11}B decoupling. The ^{11}B resonance is a broad doublet ($^1J_{HH}$ 96 Hz) in acetone-d_6. The ^{11}B chemical shift is very sensitive to the presence of a methyl substituent and shifts from δ −1.3 ppm (*vs.* $BF_3(OEt_2)$) in **3 a** to δ −8.0 ppm in **3 b**. In contrast, the B*H* shift is insensitive to substituents on the pyridine ring and coordination of diamagnetic metals. TGA shows that desolvation occurs above 100 °C (for acetone, isopropanol and water) but cage decomposition is not observed below *ca.* 420 °C for the parent cage **3 a**.

In the X-ray crystal structures of K_2(Cage-**3 a**) (Figure 2) and K_2(Cage-**3 b**) (Figure 3), three *bis*(pyrazolyl)pyridine arms span the two boron centres.[18] The coordination environment at

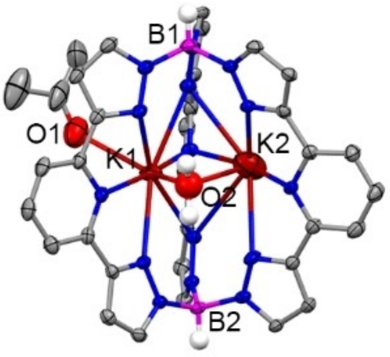

Figure 2. Ellipsoid plot (50 %) of K_2(Cage-**3 a**) (hydrogen atoms on carbon omitted for clarity).

boron is typical of a *tris*(pyrazolyl)borate. What makes these cages especially interesting is that the distance between the centroid of the nine inward-pointing N donors and the pyridine N atoms is 3.3 Å. This distance is well-suited to binding large metals such as lanthanides (discussed below), actinides, barium and lead.

The dipotassium complex of cage **3 a** absorbs strongly in the UV as expected ($\lambda_{max\text{-}MeOH}$ 238 nm; ε 113,000 $L\,mol^{-1}\,cm^{-1}$); excitation at 262 nm produces fluorescence emission at 360 nm. Acid-base titration in an 80 : 20 methanol:water solution results in a shift in the emission maximum to 405 nm between approximately pH 7 and 3 followed by a second shift to *ca.* 415 nm between pH 2.5 and −0.2 (*see* Supporting Information). These changes are attributable to the first and second protonations of **3 a**; approximate first and second pK_a values for the protonated cages are estimated to be 2.0 and 3.9, respectively.[19] This shift results in distinctly blue emission on UV excitation of the protonated cages while the parent cage is very faint violet. Cage-**3 a** is stable to pH −0.2 for at least 2–3 h but it rapidly degrades at pH > 8.5 in this medium suggesting that it will display ample stability at physiological pH.

Reaction of K_2(Cage-**3 a**) with $Ln(NO_3)_3(H_2O)_x$ (Ln=Y) or $LnOTf_3$ (Ln=Ce, Tb, Y, La) in acetone solution results in rapid precipitation (0–30 min) of Ln(**3 a**)X as their hydrated acetone complexes (Ln=Ce, **4-OTf**; Tb, **5-OTf**; Y, **6-NO$_3$**, **6-OTf**; La, **7-OTf**), Scheme 2. The Ce nitrate complex, **4-NO$_3$**, can be prepared from the Ce(IV) precursor, $(NH_4)_2[Ce(NO_3)_6]$. Acetone of solvation is readily removed under vacuum at 50–100 °C overnight but the water of solvation is not readily removed. The identity of the $[Ln(\mathbf{3a})]^+$ cation is uniquely identified by the ESI-MS isotope pattern (*see* Supporting Information) and elemental analyses (nitrate complexes) confirm the hydrate formulations.

Single crystals of **4-NO$_3$** (Ce) and **6-NO$_3$** (Y) were grown from acetone or dmso, respectively; thermal ellipsoid plots for these complexes are shown in Figures 4 and 5. In both complexes, the metal is located off-centre and resides in a cleft between two arms with coordination by all six N of those arms. Both complexes also contain coordinated water molecules (two for

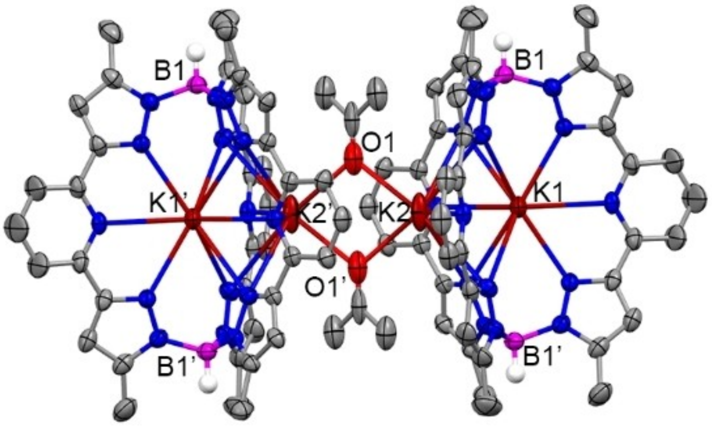

Figure 3. Ellipsoid plot (50 %) of dimeric K_2-Cage-**3 b** (hydrogen atoms on carbon omitted for clarity).

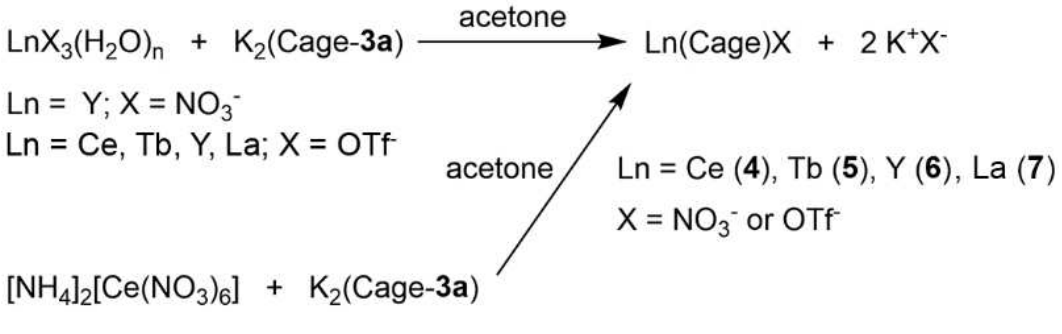

Scheme 2. Preparation of yttrium and lanthanide complexes of cage **3 a**.

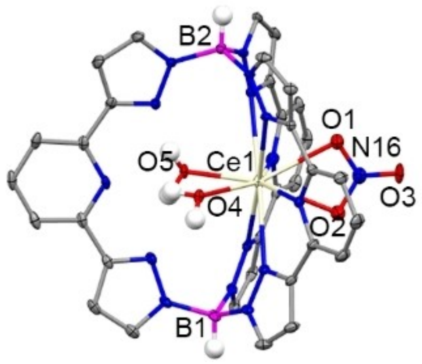

Figure 4. Thermal ellipsoid plot (50 %) of **4-NO$_3$** (non-coordinating acetone and all hydrogens on carbon omitted for clarity).

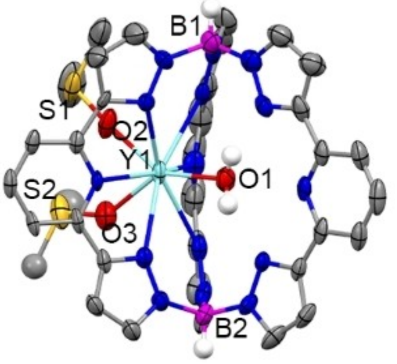

Figure 5. Thermal ellipsoid plot (50 %) for **6-NO$_3$** (non-coordinating, disordered nitrate anion and all hydrogens on carbon omitted for clarity).

Ce, one for Y) hydrogen bonded to the pyridine of the non-coordinating arm. These waters are thus internal to the cage structure so the observation that they are not readily lost on heating is not surprising. The structures differ in coordination of the nitrate counterion. In the case of Ce complex, **4-NO$_3$**, the nitrate is coordinated in typical bidentate fashion while in the Y complex, **6-NO$_3$**, it is non-coordinating and replaced within the coordination sphere by two O-coordinated dmso molecules. Thus the coordination number at the metal is 10 for Ce and 9 for Y. The metal-bonded arms are warped out of planarity, as was observed in K_2(Cage-**3 a**).

The ^{1}H NMR spectra of **4-OTf**, **6-NO$_3$**, **6-OTf** and **7-OTf** show a symmetrical environment that does not match that observed for **4-NO$_3$** or **6-NO$_3$** in the solid state. In contrast, both the cerium nitrate complex **4-NO$_3$** and the terbium triflate complex **5-OTf** clearly show two sets of arm resonances in 2:1 ratio (**5-OTf**, Figure 6) that *are* consistent with the crystal structures of **4-NO$_3$** and **6-NO$_3$**. The most likely explanation for this behaviour is a fluxional process where the metal migrates rapidly between all three clefts on the NMR timescale for Ce (**4-OTf**), Y (**6-OTf** or **6-NO$_3$**) and La (**7-OTf**). The coordinated nitrate in **4-NO$_3$** presumably hinders rapid migration while the much larger chemical shift differences for Tb (**5-OTf**) places this complex in the slow exchange regime.

Terbium cage **5-OTf** shows the typical green Tb^{3+} emission spectrum when excited at 335 nm in 20 % dmso in water solution. In contrast, the emission is almost completely quenched for $Tb(OTf)_3$ in this solvent mixture, demonstrating the solvent shielding effects of the cage (*see* Supporting Information). This suggests **5** may also be interesting as a fluorescent tag when attached to biomolecules.

The uptake of lanthanide ions by **3 a** in acetonitrile is extremely rapid at room temperature, even at the low concentrations of ESI-MS (10^{-5} M) as illustrated by pressurized sample infusion ESI-MS (Figure 7).[20] The ESI-MS spectra of **4–7** in acetonitrile and **7** in an 80:20 methanol:water mixture show no change over several months. Additionally, no change is observed for **7** in the presence of more than 1000 equivalents of $NaHCO_3$ in 80:20 methanol:water over one month (*see* Supporting Information). Further, there is no evidence for metal exchange over a period of more than a week when these complexes are challenged with a 250-fold excess of a different lanthanide triflate (*see* Supporting Information for **7-OTf** challenged with $Tb(OTf)_3$). These preliminary results are promising indicators that mausolate cages are tenacious chelators of large lanthanide ions.

In summary, the new mausolate clathrochelate based on the well-known *tris*(pyrazolyl)borate core displays exceptional thermal stability and resistance to air and water degradation at neutral and acidic pH. The rapid uptake of lanthanide ions from

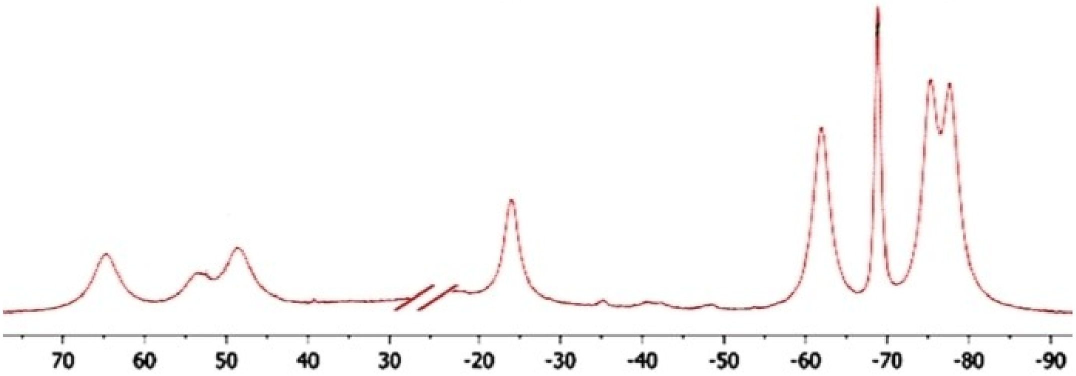

Figure 6. ^{1}H NMR (500 MHz, ppm, dmso-d_6) spectrum of Tb complex **5-OTf** (diamagnetic region omitted for clarity, one resonance not observed).

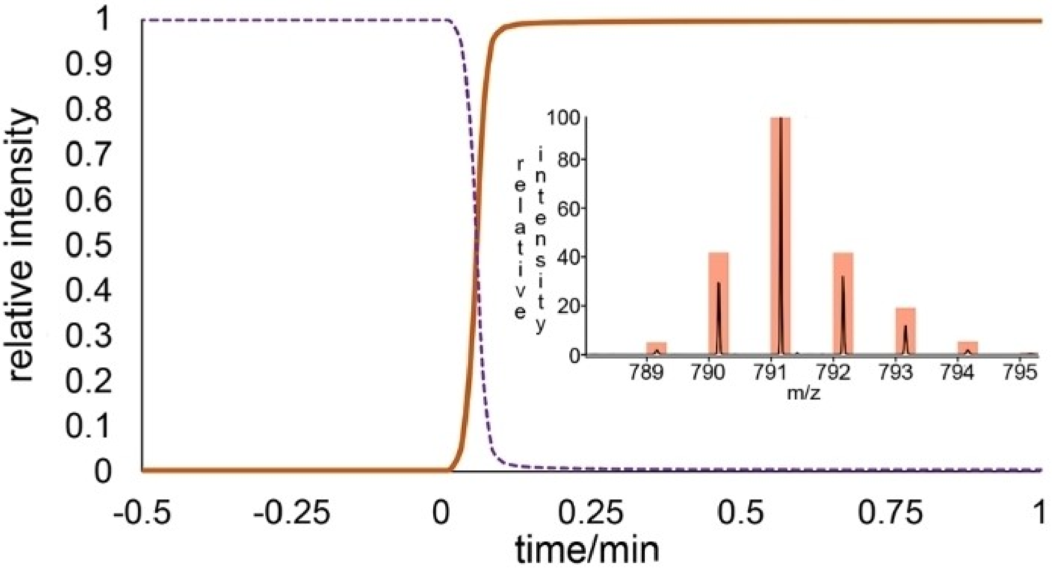

Figure 7. Uptake of Ce^{3+} ions by **3 a** monitored by pressurized sample infusion ESI MS[20] (20 μM $Ce(OTf)_3$ and K_2Cage-**3 a** in acetonitrile): orange solid line $[\mathbf{4}]^+$, purple dashed line sum of $[K_3$Cage-**3 a**$]^+$ and $[K_2H$Cage-**3 a**$]^+$; inset: observed and calculated (shaded) isotope pattern for $[\mathbf{4}]^+$.

solution at room temperature and the stability of these complexes to metal displacement make mausolates highly attractive vehicles for the delivery of large radionuclides *in vivo*. Future work to determine the stability of complexes with other metals and to functionalize the mausolate periphery are underway.

Supporting Information

Synthetic procedures, selected NMR spectra, crystallographic data, UV-Vis and fluorescence spectroscopy and ESI-MS data are given in the Supporting Information (64 pages). The authors have cited additional references within the Supporting Information.[21–28]

Acknowledgements

The authors wish to thank Dr. Charles Stone for his enthusiastic support of this work. DJB thanks U-REIF Investments for operating funds. The authors also wish to acknowledge the assistance of Chris Barr in helping obtain heteronuclear NMR (^{11}B, ^{15}N). JSM thanks NSERC and the University of Victoria for operating funds and infrastructural support.

Conflict of Interests

The authors declare no conflict of interest.

Data Availability Statement

The data that support the findings of this study are available from the corresponding author upon reasonable request.

Keywords: Clathrochelate · Cage · Chelator · Lanthanide · Borate

[1] K. Kishiro, H. Hanaoka, A. Yamaguchi, K. Ogawa, *Coord. Chem. Rev.* **2019**, *383*, 104–131.
[2] C. Muller, K. A. Domnanich, C. A. Umbricht, N. P. van der Meulen, *Br. J. Radiol.* **2018**, *91*, 20180074.
[3] *Targeted Therapies in Oncology* (Eds: G. Giaccone, J.-C. Soria), CRC Press, United States **2014**.
[4] *Monoclonal Antibody and Peptide-Targeted Radiotherapy for Cancer* (Ed: R. M. Reilly), John Wiley and Sons, Inc. **2010**, pp. 640.
[5] F. Roesch, *Radiochim. Acta* **2007**, *95*, 303–311.
[6] R. M. Pallares, R. J. Abergel, *Front. Med.* **2022**, *9*, 1020188.
[7] C. M. Patel, T. Wadas, *Molecules* **2021**, *26*, 2162.
[8] F. Brucherseifer, A. Kellenbauer, R. Malmbeck, A. Morgenstern, *J. Labelled Comp. Radiopharm.* **2019**, *62*, 794–802.
[9] *Targeted Alpha Therapy, Part 1*, in *Curr. Radiopharm*, *4* (Ed: J. Elgqvist), Bentham Science Puvlishers, Ltd. **2011**, pp. 104.
[10] D. J. Berg, WO2023/183813, **2023**. Assigned to U-REIF Investments Limited Partnership.
[11] S. Trofimenko, *J. Am. Chem. Soc.* **1967**, *89*, 3165–3170.
[12] S. Trofimenko, *J. Am. Chem. Soc.* **1967**, *89*, 3170–3177.
[13] S. Trofimenko, *Polyhedron* **2004**, *23*, 197–203.
[14] C. Pettinari, C. Santini, *'Polypyrazolylborate and Scorpionate Ligands'* in *Comprehensive Coordination II*, Vol. 1 (Eds: J. M. McCleverty, T. J. Meyer), Elsevier **2004**, pp. 159–210.
[15] M. D. Ward, J. A. McCleverty, J. C. Jeffery, *Coord. Chem. Rev.* **2001**, *222*, 251–272.
[16] C. I. Nieto, D. Sanz, R. M. Claramunt, I. Alkorta, J. Elquero, *Coord. Chem. Rev.* **2022**, *473*, 214812.
[17] a) *Clathrochelates: Synthesis, Structures and Properties* (Eds: Y. Z. Voloshin, N. A. Kastromina, R. K. Krämer), Elsevier, Netherlands **2002**; b) *Cage Metal Complexes; Clathrochelates Revisited* (Eds: Y. Z. Voloshin, I. Belaya, R. K. Krämer), Springer International Publishing, New York **2017**; c) S. M. Jansze, K. Severin, *Acc. Chem. Res.* **2018**, *51*, 2131–2147.

[18] CSD Deposition numbers 2305446 (for 3**a**), 2305447 (for 3**b**), 2305448 (for **4-NO3**) and 2305449 (for **6-NO3**) contain the supplementary crystallographic data for this paper. These data are provided free of charge by the joint Cambridge Crystallographic Data Centre and Fachinformationszentrum Karlsruhe Access Structures service.
[19] J. Catalán, R. M. Claramunt, J. Elquero, J. Laynez, M. Menández, F. Anvia, J. H. Quian, M. Taagepera, R. W. Taft, *J. Am. Chem. Soc.* **1988**, *110*, 4105–4111.
[20] G. T. Thomas, S. Donnecke, I. C. Chagunda, J. S. McIndoe, *Chemistry-Methods* **2022**, *2*, e202100068.
[21] APEX-3. Bruker AXS. Madison, Wisconsin, USA **2016**.
[22] L. Krause, R. Herbst-Irmer, G. M. Sheldrick, D. Stalke, *J. Appl. Cryst.* **2015**, *48*, 3.
[23] G. M. Sheldrick, *Acta Cryst.* **2015**, *A71*, 3.
[24] G. M. Sheldrick, *Acta Cryst.* **2015**, *C71*, 3.
[25] a) O. V. Dolomanov, L. J. Bourhis, R. J. Gildea, J. A. K. Howard, H. Puschmann, *J. Appl. Crystallogr.* **2009**, *42*, 339; b) OLEX2, OlexSys Ltd., Durham, UK **2017**.
[26] S. Parsons, H. D. Flack, T. Wagner, *Acta Cryst.* **2013**, *B69*, 249.
[27] R. W. W. Hooft, L. H. Straver, A. L. Spek, *J. Appl. Cryst.* **2008**, *41*, 96.
[28] A. L. Spek, *Acta Cryst.* **2009**, *D65*, 148.

Manuscript received: May 21, 2024
Accepted manuscript online: May 31, 2024
Version of record online: July 22, 2024